REPORT DOCUMENTATION PAGE

Form Approved
OMB No. 0704-0188

1. AGENCY USE ONLY (Leave blank)	2. REPORT DATE	3. REPORT TYPE AND DATES COVERED
	5/15/96	6/95 - 3/96

4. TITLE AND SUBTITLE
Electrochemistry of Sulfur Adlayers on the Low-Index Faces of Silver

5. FUNDING NUMBERS
N0014-94-1-0323
R & T Code 413V001

6. AUTHOR(S)
David W. Hatchett and Henry S. White

7. PERFORMING ORGANIZATION NAME(S) AND ADDRESS(ES)
Department of Chemistry
Henry Eyring Building
University of Utah
Salt Lake City, Utah 84112

8. PERFORMING ORGANIZATION REPORT NUMBER
15

9. SPONSORING/MONITORING AGENCY NAME(S) AND ADDRESS(ES)
Office of Naval Research
800 North Quincy Street
Arlington, Virginia

10. SPONSORING/MONITORING AGENCY REPORT NUMBER

11. SUPPLEMENTARY NOTES

12a. DISTRIBUTION/AVAILABILITY STATEMENT
Unclassified/Unlimited

12b. DISTRIBUTION CODE

13. ABSTRACT (Maximum 200 words)

The formation and reactivity of sulfur adlayers on single-crystal Ag electrodes ((111), (110), and (100) orientations) in aqueous solutions (pH = 13) containing HS^- is reported. Oxidative adsorption of HS^- ($Ag + HS^- \rightarrow AgSH + e^-$) occurs on all three low-index surfaces at potentials ranging between -0.5 and -0.7V of the thermodynamic value for bulk Ag_2S formation. Voltammetric and electrochemical quartz crystal measurements demonstrate that the resulting AgSH adlayer undergoes a second one-electron oxidation ($AgSH + Ag + OH^- \rightarrow Ag_2S + H_2O + e^-$) at the (111) and (110) surfaces prior to bulk Ag_2S formation, yielding an underpotential deposited Ag_2S adlayer (surface coverages (S/Ag): $\theta_{Ag(111)} = 0.46 \pm 0.02$ and $\theta_{Ag(110)} = 0.54 \pm 0.03$). In contrast, the AgSH adlayer on Ag(100) is chemically inert prior to bulk Ag_2S formation. Structural models indicate that the formation of a nearly stoichiometric Ag_2S adlayer (i.e., $\theta \sim 0.5$) is feasible on the (111) and (110) surfaces without significant reconstruction of the outermost atomic layers of the substrate, but not on the (100) surface. The results suggest that the formation of a Ag_2S monolayer is allowed only when the number density of S and Ag atoms at the interface is nearly coincident with the reaction stoichiometry.

14. SUBJECT TERMS	15. NUMBER OF PAGES
	16. PRICE CODE

17. SECURITY CLASSIFICATION OF REPORT	18. SECURITY CLASSIFICATION OF THIS PAGE	19. SECURITY CLASSIFICATION OF ABSTRACT	20. LIMITATION OF ABSTRACT
Unclassified	Unclassified	Unclassified	

OFFICE OF NAVAL RESEARCH

Contract N00014-94-1-0323

R & T Code 413v001

Technical Report No. 15

ELECTROCHEMISTRY OF SULFUR ADLAYERS ON THE LOW-INDEX FACES OF SILVER

by

DAVID W. HATCHETT AND HENRY S. WHITE

Prepared for Publication in

Journal of Physical Chemistry

University of Utah
Department of Chemistry
Salt Lake City, UT 84112

December 1995

Electrochemistry of Sulfur Adlayers on the Low-Index Faces of Silver.

David W. Hatchett and Henry S. White*
Department of Chemistry, University of Utah, Salt Lake City, UT 84112

Abstract. The formation and reactivity of sulfur adlayers on single-crystal Ag electrodes ((111), (110), and (100) orientations) in aqueous solutions (pH = 13) containing HS^- is reported. Oxidative adsorption of HS^- ($Ag + HS^- \rightarrow AgSH + e^-$) occurs on all three low-index surfaces at potentials ranging between -0.5 and -0.7V of the thermodynamic value for bulk Ag_2S formation. Voltammetric and electrochemical quartz crystal measurements demonstrate that the resulting AgSH adlayer undergoes a second one-electron oxidation ($AgSH + Ag + OH^- \rightarrow Ag_2S + H_2O + e^-$) at the (111) and (110) surfaces prior to bulk Ag_2S formation, yielding an underpotential deposited Ag_2S adlayer (surface coverages (S/Ag): $\theta_{Ag(111)} = 0.46 \pm 0.02$ and $\theta_{Ag(110)} = 0.54 \pm 0.03$). In contrast, the AgSH adlayer on Ag(100) is chemically inert prior to bulk Ag_2S formation. Structural models indicate that the formation of a nearly stoichiometric Ag_2S adlayer (i.e., $\theta \sim 0.5$) is feasible on the (111) and (110) surfaces without significant reconstruction of the outermost atomic layers of the substrate, but not on the (100) surface. The results suggest that the formation of a Ag_2S monolayer is allowed only when the number density of S and Ag atoms at the interface is nearly coincident with the reaction stoichiometry.

Submitted to *J. Phys. Chem.*, December, 1995.

Introduction. Metal oxidation reactions yielding stable films comprising a metal cation and charge-balancing anion, especially metal oxides, are of general interest in fields of catalysis, corrosion, and microelectronics device fabrication. Specifically, technologies based on metal oxidation chemistry frequently require precise control or knowledge of the morphology and electronic structure of films of molecular dimensions. During the past decade, emphasis has been placed on revealing atomic-level structural details of such thin films using high-resolution surface analytical techniques, e.g., scanning tunneling microscopy[1] and low energy electron diffraction.[2] In addition to surface structural tools, electrochemical methods are particularly well-suited to investigations of solution-phase metal oxidation since the surface oxidation state can be continuously and precisely controlled by varying the electrostatic potential of the metal/solution interface.[3-11] For example, in a recent report from this laboratory, we described the electrochemical deposition and reactivity of sulfur adlayers at Ag(111) electrodes immersed in an aqueous solution (pH 13) containing HS^-.[12] The adsorption of HS^- onto Ag surfaces represents the initial step in the growth of a thin Ag_2S layer on Ag,[13-16] a process that is representative of the oxidation of many metal surface. Our previous electrochemical studies have revealed that deposition of the first monolayer of Ag_2S proceeds through a potential-dependent mechanism involving at least two chemically distinct species of adsorbed S at the $Ag(111)/H_2O$ interface.[1] We now report details of the absorption and reactivity of HS^- on all three low-index Ag surfaces.

The formation of a sulfur adlayer at Ag(111) begins at potentials ~0.5 V negative of the thermodynamic redox potential for bulk oxidation of Ag in a HS^- solution ($E^o(Ag/Ag_2S)$ = -0.88 V vs. Ag/AgCl).[17] The results of previous coulometric, voltammetric, and in-situ electrochemical quartz crystal microbalance (EQCM) mass measurements indicate that the initial adlayer results from the reversible 1-e^- oxidative adsorption of HS^-, i.e., adsorption of HS^- is a redox

$$AgSH + e^- \rightleftharpoons Ag + HS^- \qquad (1)$$

process resulting in a AgSH surface complex.[12] At more positive potentials, but again prior to bulk Ag oxidation, the adsorbed layer is further oxidized yielding a monolayer of Ag_2S, eq. (2). The Ag/S stoichiometry indicated in eq. (2) is based on the potential-dependent

$$Ag_2S + H_2O + 1e^- \rightleftharpoons AgSH + Ag + OH^- \qquad E^o = -0.88 \text{ V vs. Ag/AgCl} \tag{2}$$

number density of S adatoms per Ag atom on the (111) surface (i.e., the surface coverage or packing density, θ) determined by in-situ EQCM and coulometric measurements.[12] Specifically, a negligible change in the mass of the adsorbed layer is observed during the second surface oxidation reaction, consistent with eq. (2) which indicates that the only anticipated mass change is that corresponding to expulsion of protons from the interface. Combining eqs. (1) and (2) yields the overall reaction for deposition of a monolayer of Ag_2S on the Ag(111) surface.

$$Ag_2S + H_2O + 2e^- \rightleftharpoons HS^- + 2Ag + OH^- \tag{3}$$

Because eq. (3) describes both bulk and surface Ag oxidation, the deposition of a monolayer of Ag_2S at potentials prior to bulk Ag oxidation is similar to the more well-studied underpotential deposition (upd) of metal atoms on a foreign metal electrode[18] (e.g., Pb deposition on Ag[19]). In the latter case, the reductive deposition of a monolayer of metal atoms ($M^{z+} + ze^- \rightleftharpoons M$) is observed at potentials positive of the thermodynamic potential for bulk metal deposition, $E^o(M^{z+}/M)$. The initial potential-dependent adsorption of anions (in metal oxidation) or cations (in upd films) are physically similar processes; however, the continued growth of metal oxidation layers, such as Ag_2S on Ag, is inherently more complex than metal deposition reactions, due to the fact that oxidative film growth requires chemical reaction between two species (bulk metal atom and solution anion) that are separated by a product film.

Adsorption of HS^- (eq. (1)) is also analogous to the oxidative adsorption of halogens on Ag (eq. (4), X = I, Br, and Cl) at potentials negative of the thermodynamic potential for bulk AgX formation.[20,21] However, the Ag/sulfur appears unique among

metal/anion adlayer systems in that the final adlayer structure results from two discrete 1-e^- oxidative steps, eqs. (1) and (2).

$$AgX + e^- \rightleftharpoons Ag + X^- \quad (4)$$

In current work, we have extended our studies of sulfur adlayers to all three low-index surfaces of Ag single-crystal electrodes. We observe that oxidative adsorption of HS^- (eq. (1)) occurs at all three surfaces at potentials negative of $E^o(Ag/Ag_2S)$. As anticipated, the potential at which HS^- adsorption occurs, and the resulting surface coverages are strongly dependent on the surface orientation of the Ag electrode. However, in addition to these expected dependencies, the chemical reactivity of adsorbed HS (eq. (2)) is surprisingly sensitive to crystallographic orientation of the Ag electrode. In particular, oxidation of AgSH to an upd Ag_2S monolayer occurs at the (111) and (110) surfaces, but not on the (100) surface. The dependence of the AgSH adlayer reactivity on crystallographic orientation is interpreted in terms of the relationship between allowed packing densities and surface reaction stoichiometry.

Experimental.

Electrochemical Cell and Apparatus. A standard one-compartment cell containing Pt and Ag/AgCl (3M NaCl) auxiliary and reference electrodes, respectively, and equipped with ports for inlet and outlet N_2 flow, was used for all experiments. All solutions contained 0.75 mM Na_2S and 0.2M NaOH. The primary S species present in this solution is hydrosulfide, HS^- (>99.99 %), as determined from the literature pK_a values for H_2S (7.02) and HS^- (17.1).[22] Solutions were purged for ~20 minutes with N_2 to remove O_2 from the solution, and a positive pressure of N_2 was maintained in the electrochemical cell. Measurements were made at 25 ± 2°C. Voltammetric data were obtained using a Princeton Applied Research Corp. (PARC) Model 173 Potentiostat and a Model 175 Universal Programmer. A Kipp and Zonen Model BD-90 x-y recorder was used to record voltammetric curves.

Electrochemical Quartz Crystal Microbalance. The EQCM is identical to that described in our earlier studies[12] and is based on a design by Ward.[23] Preparation of (111)-oriented

Ag-coated EQCM crystals, as well as detailed procedures for frequency calibration and evaluation of the mass detection limit in HS^- solutions, have been previously reported.[12]

Chemicals. All solutions were prepared using water obtained from a Barnstead "E-pure" water purification system. NaOH (Mallinckrodt, 98.8%), Na_2S (Mallinckrodt, 98.8%), NaCN (Mallinckrodt, 98.8%) were used as received.

Preparation of Ag Single Crystal Electrodes. Ag single crystals were obtained from Monocrystals Company. The exposed surface areas of the (111)-, (110)-, and (100)-oriented electrodes were 0.30 cm^2, 0.64 cm^2, and 0.64 cm^2, respectively. Each crystal was embedded into a Kel-F rod, and a Ag wire was attached to the embedded side with conductive Ag epoxy (5504N, Dupont). The electrodes were polished using progressively finer grades of alumina powder (from 1.5 μm to 0.01 μm diameter) until a mirror surface was obtained on the Ag surface. Immediately prior to voltammetric measurements, the single-crystal electrodes were chemically polished using a procedure originally described by Bewick et al.[24] Because the voltammetric response is critically dependent upon surface preparation, we briefly describe this procedure. Initially, the electrode is immersed in a freshly prepared solution containing equal volumes of aqueous 0.43 M NaCN and 20% H_2O_2/H_2O (v/v). After ~3 s, gas evolution is observed at the surface of the Ag electrode. The electrode was removed from this solution to air with a thin film of the etching solution clinging to the electrode surface. After a few seconds in air, gas evolution from the electrode surface is visible in the thin solution film. The electrode is then placed in a 0.77 M NaCN solution until visible gas evolution ceases. This procedure is repeated ~10 times until a mirror finish is obtained on the exposed Ag surface. The electrode is then washed with purified H_2O and transferred to the electrochemical cell. Reproducible electrochemical results at all three low-index faces were obtained following this procedure.

Results and Discussion.

Ag(111). The voltammetric response of the Ag(111) single-crystal electrode in an aqueous solution containing 0.75 mM Na_2S and 0.2 M NaOH is shown in Fig. 1. An anodic wave (labeled D_a) is observed on the positive-going scan at potentials slightly positive of $E^o(Ag/Ag_2S)$. This anodic wave corresponds to the oxidation of bulk Ag, leading to the deposition of a relatively thick Ag_2S film, eq. (3), as had been previously

determined using polycrystalline Ag electrodes.[13-15] Several smaller peaks can be discerned within wave D_a, suggesting that bulk deposition of Ag_2S at the Ag(111) surface occurs in a multistep process that is resolvable by voltammetric measurements. However, we have not pursued this finding. Upon reversing the direction of the potential scan, the Ag_2S layer is cathodically reduced, as evidenced by a large stripping peak (D_c) at potentials slightly negative of $E^o(Ag/Ag_2S)$. From coulometric integration of the area under the stripping wave, the thickness of the Ag_2S layer generated during this specific voltammetric experiment is estimated to be equivalent to ~8 monolayers of Ag_2S.[25] The onset of bulk Ag_2S deposition is shifted positive from $E^o(Ag/Ag_2S)$ by ca. 0.05 V, indicating a significant kinetic barrier to growth of Ag_2S on Ag(111). The irreversible nature of eq. (3) is also apparent in the relatively large potential splitting of the Ag_2S deposition and reduction waves.

At potentials negative of the bulk Ag_2S deposition and reduction wave (D_a/D_c), several smaller waves are observed that are associated with adsorption and reaction of HS^- at the Ag(111) surface. Higher-resolution voltammetry in this potential region (Fig. 2b) shows a set of three well-resolved surface waves (A_a/A_c, B_a/B_c, and C_a/C_c) with half-wave potentials, $E_{1/2}$, equal to -1.21V, -1.03, and -0.87 V vs. Ag/AgCl, respectively (where $E_{1/2} = (E_{pc} + E_{pa})/2$, and E_{pc}/E_{pa} are the cathodic/anodic peak potentials). All three surface voltammetric waves are absent in the voltammetric response obtained in solutions containing only 0.2 M NaOH.

The voltammetric response of the Ag(111) single-crystal electrode shown in Fig. 2b is essentially identical to the responses previously reported for polycrystalline (111)-oriented Ag film electrodes deposited on mica, or quartz surfaces used for the EQCM. All three surface waves (A_a/A_c, B_a/B_c, and C_a/C_c) are observed at the polycrystalline Ag film electrodes, with $E_{1/2}$ values within 10 mV of the values obtained at the single crystal electrode. Based on previous experimental studies employing mica/Ag(111) and EQCM/Ag(111) electrodes (detailed in ref. 12), we have assigned waves A_a/A_c and B_a/B_c to oxidative adsorption of HS^- (eq. (1)), resulting in the formation of the AgSH adlayer. Wave C_a/C_c corresponds to subsequent oxidation of the AgSH adlayer (eq. (2)), producing a complete Ag_2S upd layer prior to bulk oxidation of Ag. Briefly, key evidence supporting this interpretation is obtained from in-situ EQCM measurements of the

interfacial mass changes associated with each voltammetric wave. The frequency response of the EQCM/Ag(111), obtained under identical experimental conditions as those used to measure the voltammetric response at the Ag(111) single-crystal electrode, is reproduced in Fig. 2a. A reversible 2.15 ± 0.30 Hz (2σ) frequency shift is observed when the potential is scanned through voltammetric waves A_a/A_c and B_a/B_c, consistent with these waves corresponding to the reversible oxidative adsorption of HS^-. In comparison, a negligibly small frequency change is observed in the potential range of wave C_a/C_c, clearly demonstrating that this wave is not associated with a significant increase in the interfacial mass.

The Sauerbrey equation (eq. (5)) allows the frequency response of the EQCM, Δf, to be quantitatively related to the interfacial mass change, Δm.

$$\Delta f = -2f_o\Delta m / A\left(\mu_q\rho_q\right)^{1/2} \qquad (5)$$

In eq. (5), f_o is the parent resonance frequency of the crystal (~5 x 10^6 Hz), A is the area of shear motion (0.178 cm^2), and μ_q and ρ_q are the shear modules (2.947 x 10^{11} g cm^{-1} s^{-1}) and density (2.648 g cm^{-3}) of quartz, respectively. Using these values, the observed 2.15 ± 0.30 Hz frequency shift for waves A_a/A_c and B_a/B_c corresponds to an adsorbed mass of 3.8 ± 0.5 x 10^{-8} g/cm^2, or assuming that HS^- is the adsorbing species, to a surface coverage, Γ_{HS}, of 1.19 ± 0.16 x 10^{-9} mol/cm^2. In comparison, coulometric integration of the anodic (or cathodic) peaks of waves A_a/A_c and B_a/B_c yields Γ_{HS} = 1.16 x 10^{-9} mol/cm^2, assuming a 1-e^- oxidation, eq. (1). The excellent agreement between the values of Γ_{HS} determined by coulometry and EQCM mass measurements strongly supports our contention that waves A_a/A_c and B_a/B_c result from oxidative adsorption of HS^-, eq. (1). The fact that two waves are associated with interfacial mass changes (A_a/A_c and B_a/B_c) suggests that at least two energetically-distinct sites of HS^- adsorption exist at the (111) surface.

Further experimental support of our assignment of waves A_a/A_c and B_a/B_c to eq. (1) and wave C_a/C_c to eq. (2) is based on the dependence of the magnitude and shapes of these waves on the voltammetric scan rate. The peak currents associated with waves A_a/A_c and B_a/B_c at the single-crystal (111)-oriented electrode increase linearly with scan rate (ν)

for $30 < \nu < 100$ mV, Fig. 3, consistent with rapid establishment of an equilibrium surface coverage of HS on the voltammetric time scales. The symmetry of the anodic and cathodic peaks of each of these waves, which is independent of scan rate, also suggests that an equilibrium surface coverage is maintained throughout this potential region. In comparison, the peak splitting of wave C_a/C_c is significant, e.g., 50 mV at $\nu = 100$ mV/s, Fig. 2b, and increases markedly with increasing scan rate. Furthermore, we find that the magnitude of wave C_a/C_c is not proportional to ν, but rather to $\nu^{2/3}$, Fig. 3. Both of these latter observations are consistent with the AgSH-to-Ag_2S adlayer transition (eq. 2) occurring by a two-dimensional nucleation and growth process.[26] The results suggest that the oxidation of the AgSH layer to a Ag_2S layer results in a more ordered layer, analogous to potential-dependent order/disorder transitions determined by LEED for halogen adsorption on Ag(111).[27]

Coulometric integration of the anodic peaks of the three voltammetric waves (A_a, B_a, and C_a) leading to the formation of the upd Ag_2S layer yields a charge of 204 ± 10 $\mu C/cm^2$. Assuming $n = 2$ for the overall deposition of the upd Ag_2S adlayer (eq. (3)) allows the surface coverage, $\theta_{(111)}$, (i.e., the ratio of S atoms per Ag(111) surface atom) to be computed as 0.46 ± 0.02. The corresponding value determined from the EQCM/Ag(111) measurement is 0.52 ± 0.07, within error of the electrochemical results. Values of $\theta_{(ijk)}$ are used in a later section in proposing structures for the Ag_2S adlayer for each surface orientation.

Ag(110). The voltammetric response of the Ag(110) single-crystal electrode in HS^- solutions is qualitatively similar to that described above for Ag(111) electrodes. Oxidation of bulk Ag occurs at potentials slightly positive of $E^o(Ag_2S/Ag)$, resulting in a multilayer Ag_2S film that can be readily reduced off at potentials slightly negative of $E^o(Ag_2S/Ag)$. Four voltammetric waves (A_a/A_c, B_a/B_c, B_a'/B_c', and C_a/C_c) corresponding to adsorbed HS are observed with $E_{1/2}$ values of -1.36, -1.23, -1.18, and -1.09 V vs. Ag/AgCl, Fig. 2c. The close similarity of the voltammetric responses for Ag(111) and Ag(110) electrodes clearly suggests that waves A_a/A_c and C_a/C_c for both electrodes are associated with the same chemical processes. Wave B_a/B_c at the Ag(110) surface, however, appears split into two waves (B_a/B_c and B_a'/B_c') at the Ag(110) surface. Adsorption of HS^- at the Ag(110)

surface begins at potentials ~150 mV negative than on the Ag(111) surface. This shift most likely reflects the difference in the work function (Φ) of these two surfaces ($\Phi_{(111)}$ = 4.74 eV and $\Phi_{(110)}$ = 4.52 eV[28]).

The scan rate dependencies of the magnitude and shape of the voltammetric waves associated with the Ag(110) electrode are identical to that observed for the Ag(111) electrode. Waves A_a/A_c, B_a/B_c, and B_a'/B_c' increase linearly in relation to ν, with minimal peak splitting up to ν = 250 mV/s, Fig. 3. Wave C_a/C_c shows a pronounced peak splitting at higher scan rates, and the peak currents for this wave are proportional to $\nu^{2/3}$, rather than ν.

Based on the similarities in the voltammetric behaviors of the (111) and (110)-oriented electrodes, we assign waves A_a/A_c, B_a/B_c, and B_a'/B_c' to oxidative adsorption of HS^-, eq. (1). Similarly, wave C_a/C_c is assigned to the oxidation of the AgSH adlayer, yielding a Ag_2S adlayer, eq. (2). Coulometric integration of all four voltammetric waves yields a surface charge density of 145 $\pm$ 8 $\mu C/cm^2$. Assuming that Ag_2S is the final adlayer structure, the surface coverage on the (110) surface, $\theta_{(110)}$, is computed to be 0.54 $\pm$ 0.03.

Ag(100). The voltammetric response of the Ag(100) electrode in the 0.75 mM Na_2S/0.2M NaOH solution is presented in Fig. 2d. Similar to observations at the (111)- and (110)-oriented electrodes, the deposition and stripping of a multilayer film of Ag_2S occurs at potentials centered on $E^o(Ag_2S/Ag)$. The shape of this bulk wave is qualitatively similar to wave D_a/D_c for the Ag(111) electrode, Fig. 1. The voltammetric behavior associated with adsorbed HS^- at the (100) surface, however, is considerably different from the responses at either the (111) or (110) surface. Only two waves, A_a/A_c and B_a/B_c, with $E_{1/2}$ values of -1.39 and -1.21 V vs. Ag/AgCl, respectively, are observed prior to bulk Ag_2S deposition. Both of these voltammetric waves display scan rate dependencies characteristic of oxidative adsorption of HS^-, Fig. 3, analogous to waves A_a/A_c and B_a/B_c at the (111)- and (110)-oriented electrodes. Specifically, the peak currents for these two symmetrically-shaped wave increase in proportion to ν, and there is minimal peak splitting at higher scan rates. In addition, the initial adsorption of HS^- on the (100) surface is shifted negative by ~180 mV with respect to adsorption on the (111) surface, consistent

with literature values of the work functions of these two surfaces ($\Phi_{(111)}$ = 4.74 eV and $\Phi_{(100)}$ = 4.64 eV).[27]

Based on the above experimental evidence, we assign waves A_a/A_c and B_a/B_c to the oxidative adsorption of HS^-. Integration of the current associated with the anodic peaks of waves A_a/A_c and B_a/B_c yields 54 $\pm$ 4 $\mu C/cm^2$, equivalent to an HS coverage, Γ_{HS} = 5.6 $\pm$ 0.4 x 10^{-10} mol/cm^2, or a sulfur surface coverage, $\theta_{(100)}$, of 0.28 $\pm$ 0.02.

The most interesting feature of the voltammetric response of the Ag(100) electrode is the clear absence of a wave corresponding to oxidation of the AgSH adlayer. In contrast to the Ag(111) and Ag(110) electrodes, which display a well defined voltammetric wave (C_a/C_c) corresponding to the formation of an upd Ag_2S adlayer, the Ag(100) electrode response is featureless at potentials intermediate between oxidative adsorption of HS^- and the deposition of bulk Ag_2S, Fig. 2. These results unequivocally demonstrate that the Ag_2S adlayer is energetically unfavorable relative to bulk Ag_2S on the (100) surface, but not on the (111) or (110) surfaces. This difference in surface energetics is clearly associated with differences in the atomic arrangement of sulfur adatoms on the three crystallographic surfaces, a point that is discussed below in more detail.

Proposed Sulfur Adlayer Structures. Fig. 4 shows proposed models of the sulfur adlayer structures on the three low-index faces of Ag. The coverages of sulfur adatoms indicated in these drawings are consistent with the measured values determined by coulometry ($\theta_{(111)}$ = 0.46 $\pm$ 0.02, $\theta_{(110)}$ = 0.54 $\pm$ 0.03, $\theta_{(100)}$ = 0.28 $\pm$ 0.02). Admittedly, the electrochemical measurements presented in the previous sections do not directly provide structural details of the sulfur adatom position relative to the lattice of Ag atoms. Atomic level details of these adlayer structures, in contact with the electrolyte solutions, require in-situ surface-sensitive structural analysis using, for instance, STM or surface extendend X-ray adsorption fine structure measurements (SEXAFS). However, consideration of the adlayer structures is necessary as a guide in order to rationalize (*i*) the differences in the $\theta_{(ijk)}$ values, and (*ii*) the observation that a Ag_2S adlayer is energetically favorable on the (111) and (110) surfaces at potentials negative of $E^o(Ag_2S/Ag)$, but not on the (100) surface.

The in-situ EQCM mass measurements on Ag(111) surfaces demonstrate that a negligible increase in interfacial mass occurs upon oxidation of AgSH to Ag_2S. Thus, $\theta_{(ijk)}$ values are independent of the whether a AgSH or Ag_2S adlayer is being considered. However, the models in Fig. 4 correspond to full S monolayer coverages which are obtained at potentials positive of the B_a/B_c wave for the (111)- and (100)-oriented electrodes, and at potentials positive of wave B_a'/B_c' for the (110)-oriented electrode.

A ($\sqrt{7}$ x $\sqrt{7}$)R10.9 adlayer structure is proposed for the Ag(111) surface, corresponding to a theoretical surface coverage, $\theta_{(111)}$, of 0.44. The corresponding value obtained from integration of the voltammetric wave is 0.46 ± 0.02. The ($\sqrt{7}$ x $\sqrt{7}$)R10.9 structure, in which S adatoms occupy three-fold hollow and top sites, has been reported for sulfur adlayers obtained in ultra-high vacuum by dosing Ag(111) with H_2S.[29] Although this latter result supports our assignment, the adlayer structures in the liquid and vacuum environments need not necessarily be coincident, due to the interactions of solvent and electrolyte ions with the surface. Preliminary attempts at in-situ STM imaging of mica/Ag(111) electrodes under potential control in the Na_2S/NaOH solution have not been successful in revealing the adlayer structure. However, ex-situ examination of the Ag(111) surface after deposition of a Ag_2S adlayer shows a hexagonal arrangement of sulfur adatoms separated by ~4.6 Å,[30] consistent with the theoretical value of 4.56 Å for the model proposed in Fig. 4.

A c(2x3) adlayer structure at the Ag(110) surface is shown in Fig. 4. This structure corresponds to $\theta_{(110)} = 0.5$, in agreement with experimental value of 0.54 ± 0.03. In drawing the adlayer structure, we have place the S adatoms in two-fold sites along the outermost rows of Ag atoms, which, in the absence of surface reconstruction, would appear to be the most energetically-favored position of adsorption.

The c(2x4) adlayer structure proposed in Fig. 4 for the (100) surface corresponds to a theoretical surface coverage of 0.25, in reasonable agreement with the experimental value of 0.29 ± 0.02. The surface coverage is a factor of ~2 lower on the (100) surface than on the other two low-index faces of Ag, a finding that must result from repulsive lateral interactions between sulfur atoms on the (100) surface. The ionic (1.84 Å)[31] and van der Waals (~1.8Å)[32] radii for S are both significantly larger that the atomic radius of Ag (1.44 Å).[33] Thus, it is not surprising that the $\theta_{(ijk)}$ values are considerably less than

unity on all three low index surfaces. The nearest-neighbor distances corresponding to the periodic adlayer structures shown in Fig. 4 are 4.56 Å (111), 4.99 Å (110), and 6.46 Å (100), each significantly greater that the ionic or van der Waals radii of S. Other common adlayer structures on the Ag(100) surface which correspond to higher surface coverages, would yield nearest-neighbor distances that are considerably shorter. For instance, a c(2 x 2) adlayer model would result in a nearest-neighbor distance of 4.08 Å, corresponding to the S adatoms being within ~0.2 Å of each other. Such a densely packed structure would be energetically unfavorable due to large repulsive adsorbate-adsorbate interactions.

The observation that the AgSH adlayer can not be further oxidized to an upd Ag_2S adlayer at the (100) surface is interpreted as being related to the low surface coverage on this surface. In the previous report of Ag_2S adlayer formation on mica/Ag(111),[12] it was shown that voltammetric wave C_a/C_c, corresponding to the AgSH-to-Ag_2S transition, is completely absent when the surface coverage of HS was lowered below a critical value ($\theta \sim 0.32$). In these previous experiments, submonolayer coverages of HS were obtained by lowering the concentration of HS^- in the contacting solution. The results presented above indicate that the HS surface coverages are sufficiently large on the (111) and (110) surfaces to allow the oxidative AgSH-to-Ag_2S transition. The most probable reason for the existence of a critical surface coverage is that the Ag_2S adlayer has a long-range crystalline order, stabilized by electrostatic interactions within the two-dimensional Ag_2S array (similar to that in bulk solids, e.g., Ag_2S). This lattice energy may not be available when the sulfur surface coverage is sufficiently low, a situation corresponding to sub-monolayer coverages on the (111) surface[12], or full monolayer coverage on the (100) surface.

Conclusion.

Reversible oxidative adsorption of HS^- from basic solutions occurs on all three low-index Ag surfaces. Combined coulometric and EQCM measurements of the interfacial charge and mass, respectively, associated with adsorption of HS^- at Ag(111) electrodes indicates that adsorption is a 1-e^- redox process, consistent with the formation of a AgSH adlayer. The multiwave voltammetric pattern for HS^- adsorption indicates that multiple and energetically-distinct adsorption sites exist on each crystallographic suface. Future investigations using in-situ structural methods will be required to determine the potential

dependent adlayer structures. In addition, we have shown that the oxidation of the AgSH adlayer to an upd Ag_2S adlayer occurs at the (111) and (110) surfaces, but not at the (100) surface. The voltammetric response associated with this redox transition displays features characteristic of nucleation and growth of an ordered two-dimensional phase. Our results suggest that the formation of the Ag_2S adlayer is energetically favored at high surface coverages, due to the lattice energy stabilization of the ordered two-dimensional Ag_2S phase.

Acknowledgments. We gratefully acknowledge helpful discussions with Keith Stevenson and Dr. Xiaoping Gao. This work was supported by the Office of Naval Research.

References.

1. (a) Gao, X.; Zhang, Y.; Weaver, M.J. *J. Phys. Chem.* **1992**, *96*, 415; (b) Hachiya, T.; Itaya, K. *Ultramicroscopy* **1992**, *42*, 445; (c) Kwetkus, B.A.; Sattler, K. *Ultramicroscopy* **1992**, *42-44*, 749; (d) Eierdal, L.; Besenbacher, F.; Laegsgaard, E.; Stensgaard, I. *Ultramicroscopy* **1992**, *42-44*, 505; (e) Oshio, T.; Sakai, Y.; Moriya, T. *Ultramicroscopy* **1992**, *42-44*, 744; (f) Bao, X.; Barth, J.V.; Lehmpfuhl, G.; Schuster, R.; Uchida, Y.; Schlögl, R.; Ertl, G. *Surf. Sci.* **1993**, *284*, 14; (g) Jensen, F.; Besenbacher, F.; Laegsgaard, E.; Stensgaard, I. *Phys. Rev. B* **1990**, *42*, 9206.
2. (a.) Yamada, T.; Batina, N.; Itaya, K. *Surf. Sci.* **1995**, *335*, 204; (b) Laguren-Davidson, L.; Lu, F.; Salaita, G.N.; Hubbard, A.T. *Langmuir* **1988**, *4*, 224.
3. Dickertmann, D.; Schultze, J.W.; Vetter, K.J. *J. Electroanal. Chem. Interfacial Electrochem.* **1974**, *55*, 429.
4. (a) Hubbard, A.T. *Langmuir* **1990**, *6*, 97; (b) Hubbard, A.T. *Chem. Rev.* **1988**, *88*, 633.
5. Gao, X.; Zhang, Y.; Weaver, M.J. *Langmuir* **1992**, *8*, 668.
6. Gao, X.; Weaver, M.J. *J. Am. Chem. Soc.* **1992**, *114*, 8544.
7. (a) Gao, X.; Weaver, M.J. *J. Phys. Chem.* **1994**, *98*, 8086. (b) Weaver, M.J.; Gao, X. *Ann Rev. Phys. Chem.* **1993**, *44*, 459.

8. Mandler, D.; Bard, A.J. *J. Electrochem. Soc.* **1990**, *137*, 1079.
9. Magnussen, O.M.; Hagebock, J.; Hotlos, J.; Behm, R.J. *Faraday Discuss.* **1992**, *94*, 329.
10. Sneddon, D.D.; Sabel, D.M.; Gewirth, A.A. *J. Electrochem. Soc.* **1995**, *142*, 3027.
11. Valette, G.; Parsons, R. *J. Electroanal. Chem. Interfacial Electrochem.* **1986**, *204*, 291.
12. Hatchett, D.W.; Gao, X.; Catron, S.W.; White, H.S. *J. Phys. Chem*, in press.
13. Horanyi, G.; Vertes, G. *Electrochim. Acta* **1986**, 31, 1663.
14. Birss, V.I.; Wright, G.A. *Electrochim. Acta* **1982**, 27, 1.
15. Huong, C.N.V.; Parsons, R.; Marcus, P.; Montes, S.; Oudar, J. *J. Electroanal. Chem. Interfacial Electrochem.* **1981**, *119*, 137.
16. Hepel, M.; Bruckenstein, S.; Tang, G.C. *J. Electroanal. Chem. Interfacial Electrochem.* **1989**, *261*, 389.
17. Standard Potentials In Aqueous Solutions; Bard, A. J., Parsons, R., Jordon, J., Eds.; Dekker: New York, 1985.
18. (a) Jüttner, K.; Lorenz, W.J. *Zeitschrift für Physikalische Chemie Neue Folge* **1980**, *122*, 163; (b) Advances in Electrochemistry and Electrochemical Engineering; Gerischer, H.; Tobias, C.W., Eds.; Vol. 11, p. 125, John Wiley: New York, 1978.
19. Bewick, A.; Thomas, B. *J. Electroanal. Chem.* **1977**, *84*, 127.
20. Soriaga, M.P.; Chia, V.K.F.; White, J.H.; Song, D.; Hubbard, A.T. *J. Electroanal. Chem. Interfacial Electrochem.* **1984**, *162*, 143.
21. Valette, G.; Hamelin, A.; Parsons, R. *Zeitschrift für Physikalische Chemie Neue Folge* **1978**, *113*, 71.
22. Gigginback, W. *Inorg. Chem.* **1971**, *10*, 1333.
23. Ward, M.D. *J. Phys. Chem.* **1988**, *92*, 2049.
24 Bewick, A.; Thomas, B. *J. Electroanal. Chem.* **1975**, *65* , 911.
25. The structure of Ag_2S is monoclinic with angles $\alpha = \gamma = 90° \neq \beta = 125.48°$. The dimensions of the unit cell are a = 4.23 Å, b = 6.93 Å, and 9.53 Å, respectively. Using these values, the thickness of a Ag_2S layer can be calculated as d = 7.8 Å. The thickness of the bulk Ag_2S film is computed using this value and the density of Ag_2S (7.326 g/cm^3).
26. Fletcher, S.J. *J. Electroanal. Chem. Interfacial Electrochem.* **1981**, *118*, 419.

27. Salaita, G.N.; Lu, F.; Laguren-Davidson, L.; Hubbard, A.T. *J. Electroanal. Chem. Interfacial Electrochem.* **1987**, *229*, 1.
28. Albano, E.V.; Daiser, S.; Miranda, R.; Wandelt, *Surf. Sci.* **1985**, *150*, 367.
29. Shwaha, K.; Spencer, N.D.; Lambert, R.M. *Surf. Sci.* **1979**, *81*, 273.
30. Stevenson, K.J.; White, H.S. Unpublished results, University of Utah, 1995.
31. Inorganic Chemistry: Priniciples of Structure and Reactivity, 4th Ed., , Huheey, J.E.; Keiter, E.A.; Keiter, R.L.; Harper Collins, New York, 1993.
32. Bondi, A. *J. Phys. Chem.* **1964**, *68*, 441.
33. Lamble, G.M.; Brooks, R.S.; Campuzano, J.-C.; King, D.A.; Norman, D. *Phys. Rev. B* **1987**, *36*, 1796.

Figure Captions

1. Voltammetric response of Ag(111) single crystal electrode (0.64 cm^2) in a N_2-purged solution containing 0.75 mM Na_2S and 0.2 M NaOH. Scan rate = 100 mV/s. HS^- is the primary sulfur species in the solution (>99.99 %).

2. (a) Potential-dependent frequency response of a Ag(111)-coated quartz crystal in a N_2-purged solution containing 0.75 mM Na_2S and 0.2 M NaOH. Voltammetric response of (b) Ag(111), (c) Ag(110), and (d) Ag(100) single-crystal electrodes in the same solution. Scan rate: ν = 100 mV/s for (b) and (c), and ν = 200 mV/s for (d).

3. Anodic peak currents as a function of potential scan rate for each of the three low-index Ag surfaces. The exposed surface areas were: (111) 0.30 cm^2; (110) 0.64 cm^2; and (100), 0.64 cm^2.

4. Proposed packing models of HS on the three low-index surfaces of Ag.

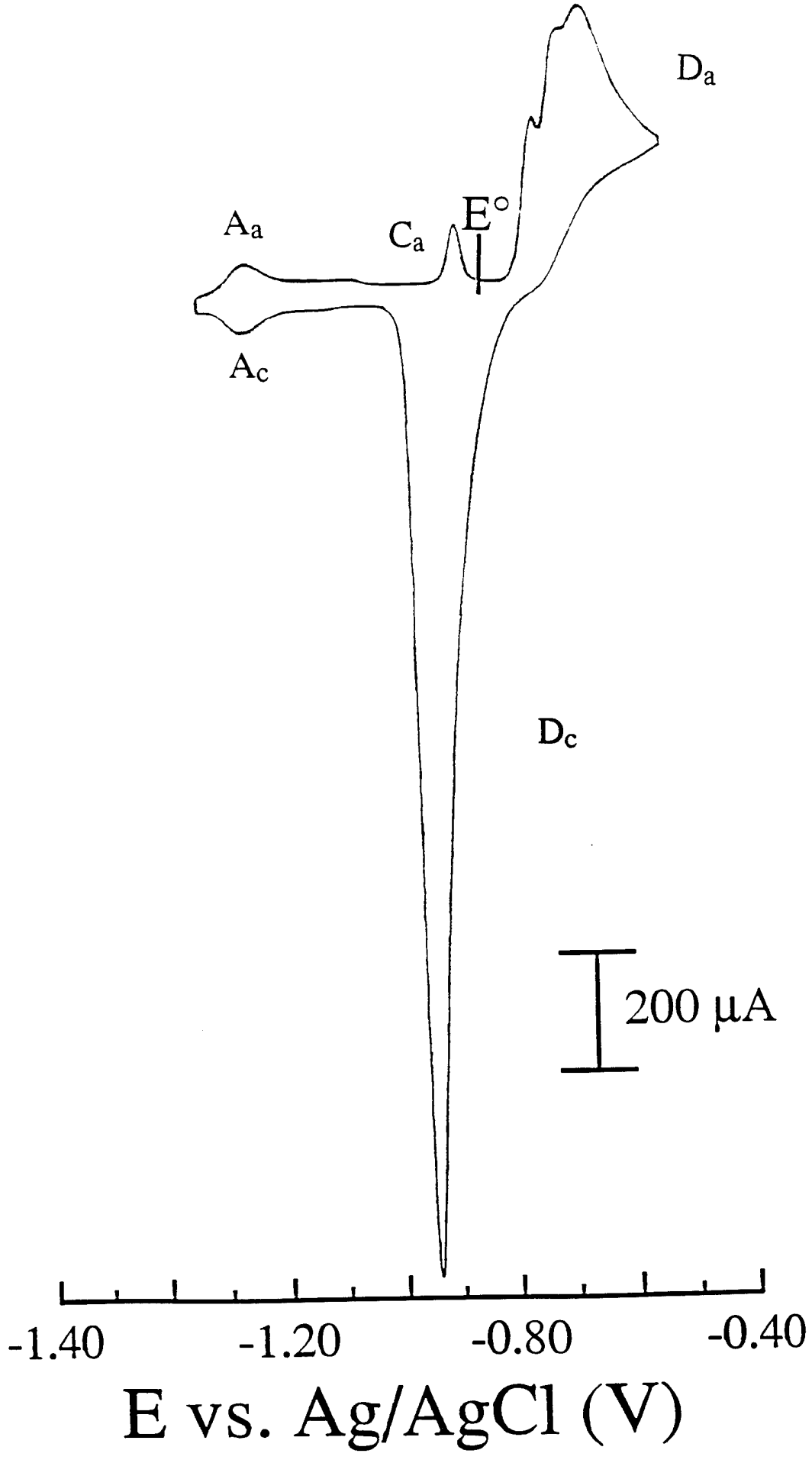
D_a
A_a
C_a
E°
A_c
D_c
200 µA
-1.40
-1.20
-0.80
-0.40
E vs. Ag/AgCl (V)

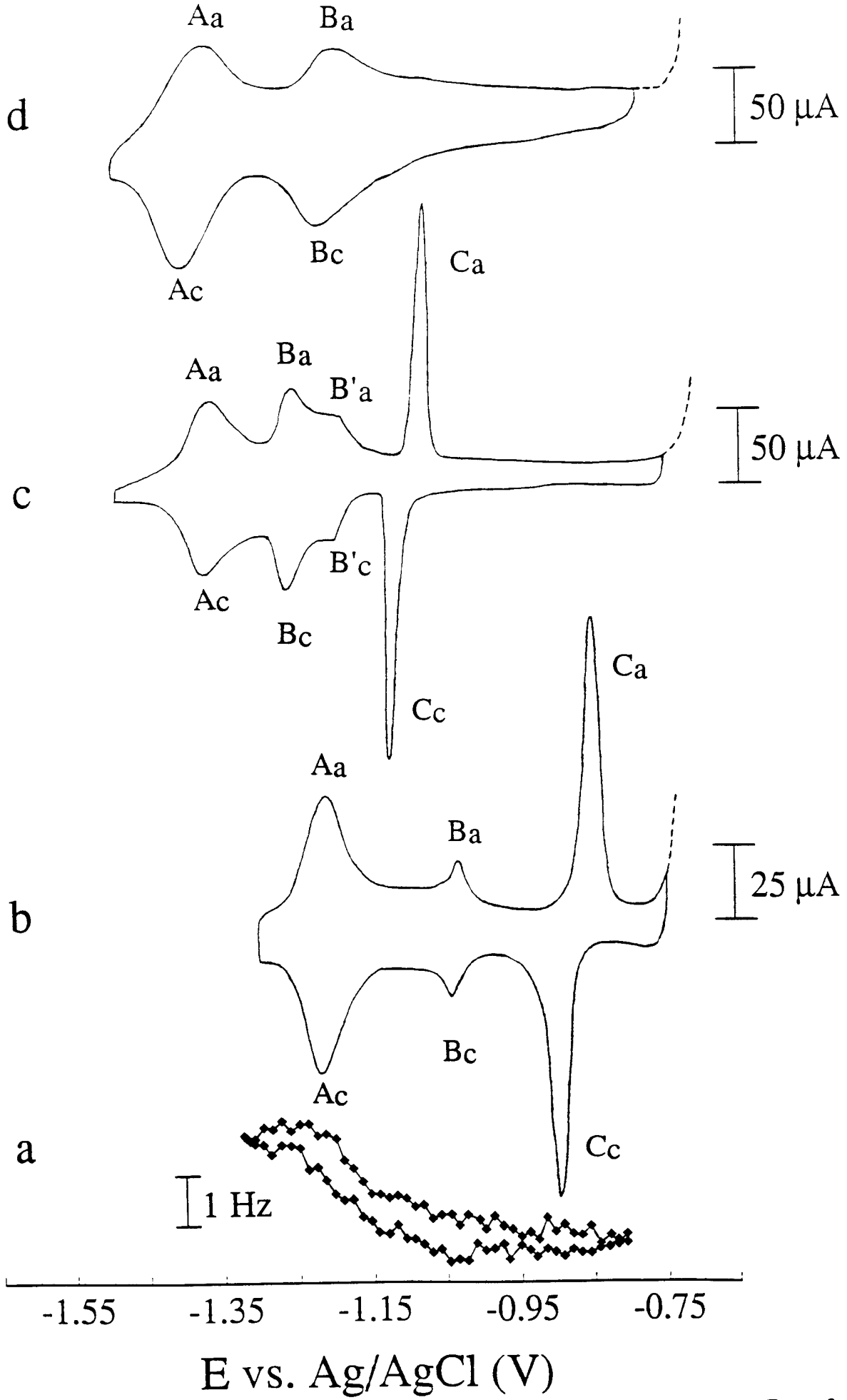
Aa
Ba
d
50 µA
Bc
Ca
Ac
Aa
Ba
B'a
50 µA
c
B'c
Ac
Bc
Cc
Ca
Aa
Ba
25 µA
b
Bc
Ac
a
Cc
1 Hz
-1.55
-1.35
-1.15
-0.95
-0.75
E vs. Ag/AgCl (V)

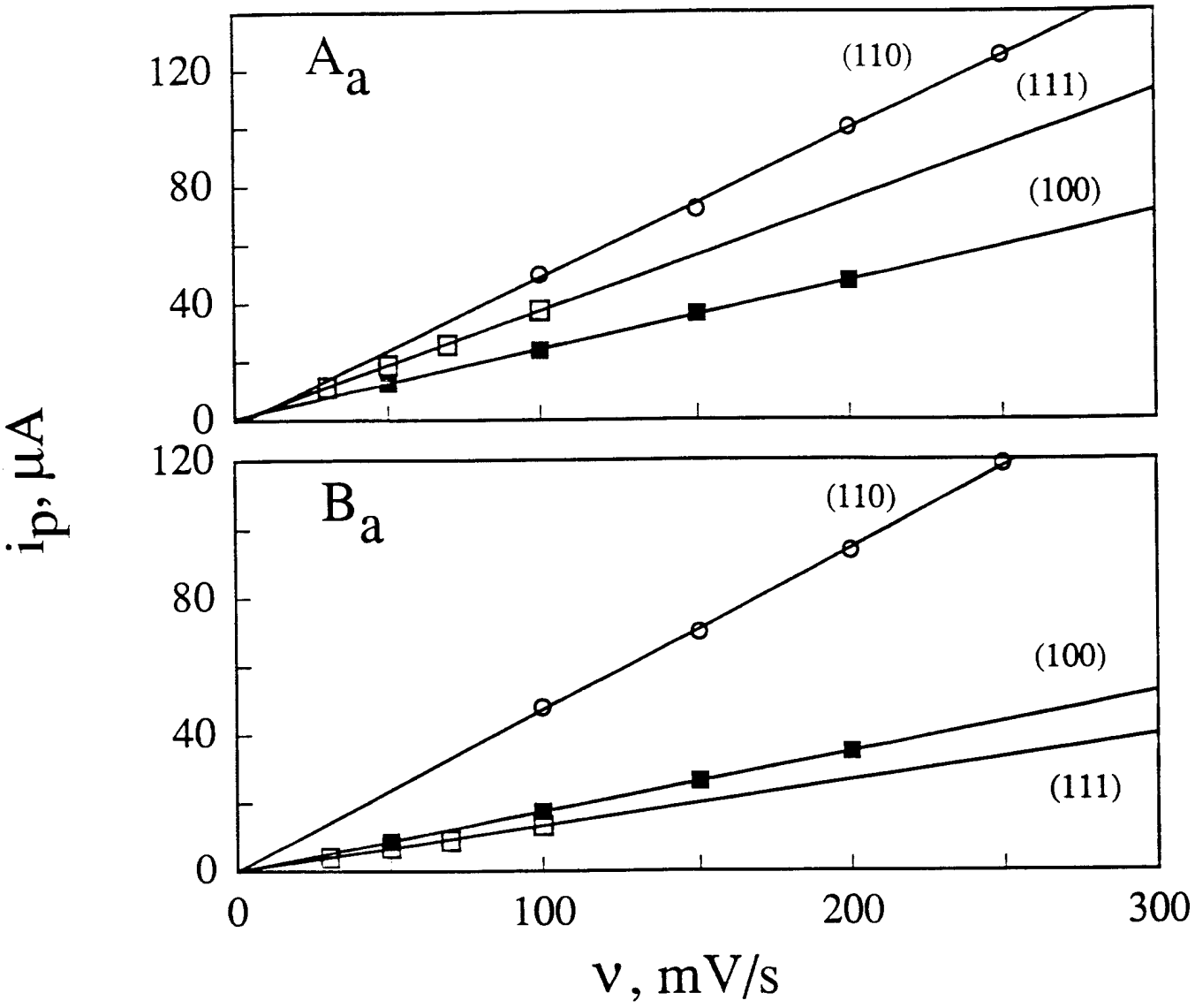
A_a
(110)
(111)
(100)
B_a
(110)
(100)
(111)
i_p, μA
120
80
40
0
0
100
200
300
ν, mV/s

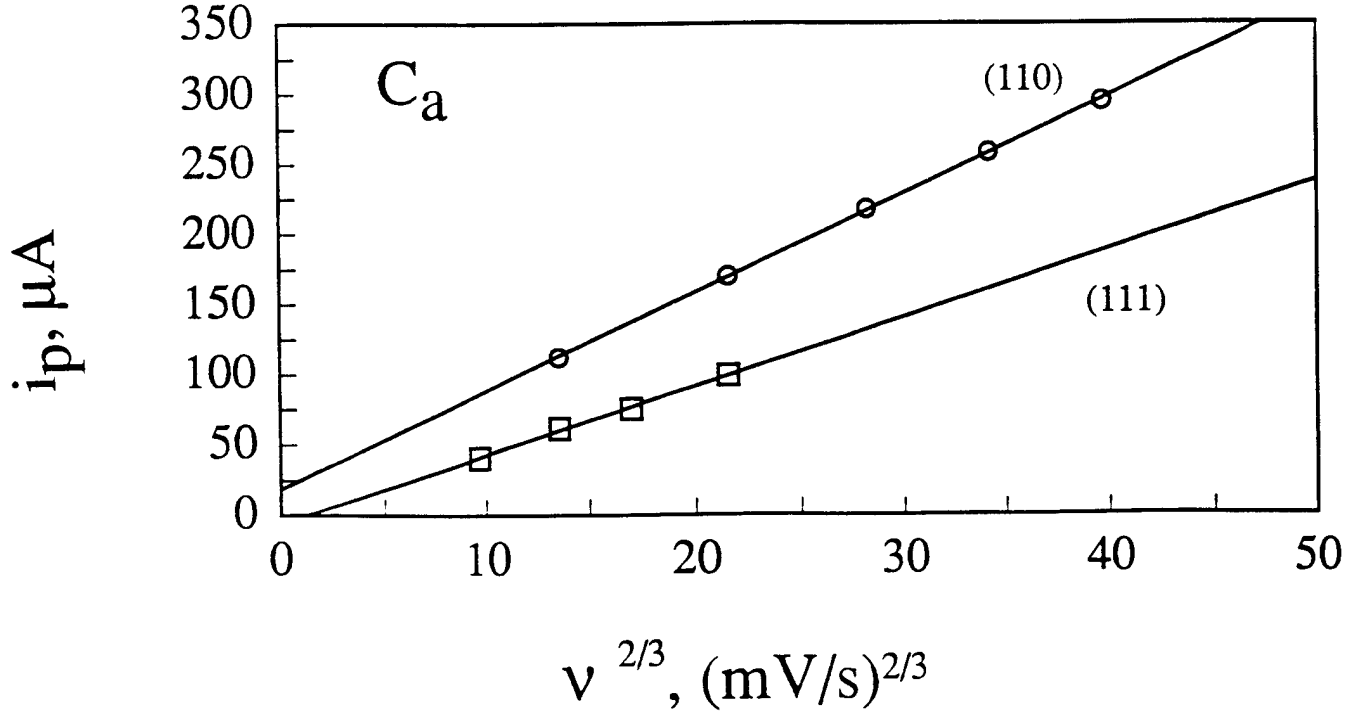
C_a
(110)
(111)
i_p, μA
350
300
250
200
150
100
50
0
0
10
20
30
40
50
ν^2/3, (mV/s)^2/3

(100)
c(2 x 4)

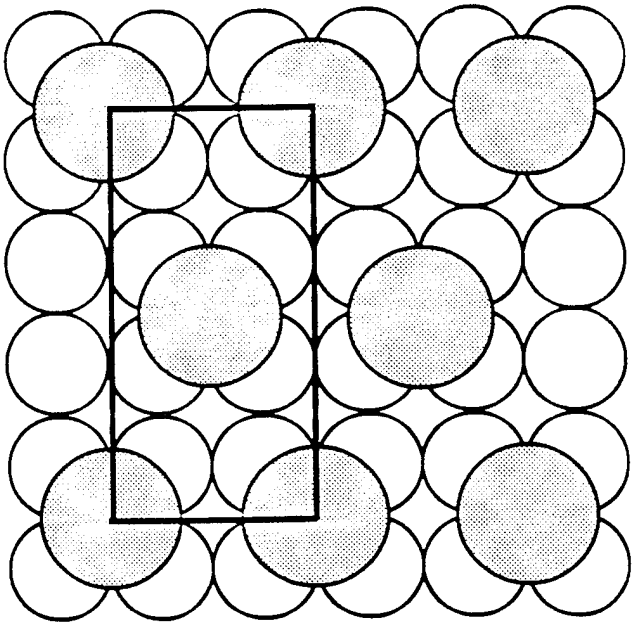

(110)
c(2 x 3)

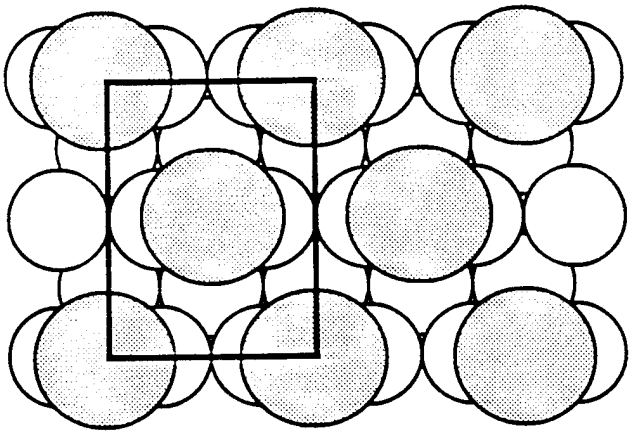

(111)
(√7 x √7)R10.9°

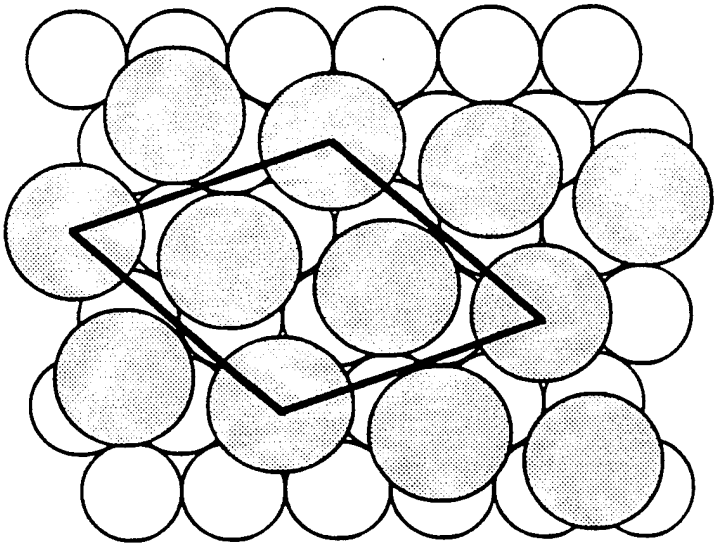

= Sulfur = Silver